Am. J. Trop. Med. Hyg., 102(2), 2020, pp. 468–475
doi:10.4269/ajtmh.19-0387

Development of a Chitosan–Vaseline Gauze Dressing with Wound-Healing Properties in Murine Models

Qing-Qing Fang,[1,2] Xiao-Feng Wang,[1,2] Wan-Yi Zhao,[1,2] Bang-Hui Shi,[2] Dong Lou,[3] Chun-Ye Chen,[2] Min-Xia Zhang,[2] Xiaozhi Wang,[4]† Lie Ma,[3]† and Wei-Qiang Tan[1,2]*†

[1]*Department of Plastic Surgery, Sir Run Run Shaw Hospital, Zhejiang University School of Medicine, Hangzhou, P. R. China;* [2]*Department of Plastic Surgery, The Fourth Affiliated Hospital, Zhejiang University School of Medicine, Yiwu, P. R. China;* [3]*Department of Polymer Science and Engineering, Zhejiang University, Hangzhou, P. R. China;* [4]*College of Information Science and Electronic Engineering, Zhejiang University, Hangzhou, P. R. China*

Abstract. Wound dressings are always needed after skin injury; however, most of the dressings still leave room for improvement. Here, we would like to develop an effective dressing with the ability to improve wound healing. A chitosan–Vaseline gauze (CVG) dressing was developed by coating the chitosan mixture and Vaseline on sterile gauze with subsequent drying. Infrared spectroscopy and electron microscopy were used to investigate the miscibility and structure of the dressing. The cytotoxicity and antibacterial nature were evaluated in vitro. The studies of water retention rate, wound healing, and tissue compatibility were carried out over a period of 14 days on full-thickness skin wounds of male Sprague–Dawley rats. It was observed that the CVG dressing demonstrated functional structure by miscibility, noncytotoxicity, and good antibacterial effects against both Gram-positive and Gram-negative bacteria. The water retention rate incresased up to 25% after applying CVG for 3 hours. Besides, CVG treatment increased angiogenesis and improved microvascular density in wounds. The wounds treated with CVG showed size deduction with new collagen aggregations similar to those in the normal dermis. All the aforementioned results suggest that CVG dressing could be a promising candidate for wound treatment.

INTRODUCTION

Skin plays a significant role in normal barrier homeostasis and preventing the invasion of microorganisms.[1] Skin lesions are traumatic events that lead to an increase of infections, fluid loss, hypothermia, locally immunocompromised regions, scarring, and a change of body image.[2,3] Among these, the growing incidence of infections remains the leading problem in wound management.[1,4] The accumulation of fluid at wound site is one of the major contributions to the bacterial invasion. Wound infections not only elicit a systemic infection (sepsis) but also inhibit the multiple processes involved in the orchestrated progression of normal wound healing. Each process involved in wound healing is affected when bacteria proliferate in a wound.[5,6]

For protection, wounds generally need to be covered with dressings immediately.[7] Effective wound dressings require not only protection of the wound from environmental irritants but also effective removal of excessive wound exudate, thus providing an optimal microenvironment to allow continuous tissue reconstruction processes.[7] In the past decades, many skin substitutes such as biologic, synthetic, and biologic–synthetic dressings have been used for the treatment of deep partial- and full-thickness wounds, but none of them is without disadvantages.[3,8] The prime requirement of an ideal dressing is that it should have the following properties: antibacterial, biocompatible, exudate absorptive, easy to apply, and promote wound healing.[9–11] These properties are primarily attributed to the functional characteristic of wound healing constituents of the dressing.

Current wound care strategies focus on the improvement of wound repair by developing better materials for the wound dressings. Different polymers, when blended together, usually achieve the functions of their constituting components in a synergistic way.[11,12] Blending of two or more polymers has become an increasingly important approach to developing new materials with new properties which could not be achieved by the individual component polymer. Chitin's derivative, chitosan, is an attractive biomaterial for wound care owing to its antibacterial, wound healing promoting, nontoxic, biocompatible, and biodegradable properties.[7,13] Chitosan has been widely used to develop dressings for wound care applications.[11,14] Vaseline (petroleum jelly), known as a lubricant, can also be used as a moisture insulator for local skin conditions characterized by tissue dehydration. Vaseline gauze (VG), which is widely used in clinics, possesses the moisture-retention ability and can reduce the pain and prevent synechia formation.[15,16] However, the disadvantage of VG is obvious by lacking the antibacterial activity, and thus limiting its clinical application.

In view of these, we aimed to create a dressing with antibacterial and wound-healing properties. Our previous work had proved that chitosan mixture could give full play to the performance of chitosan, which had obtained the China National Patent (patent number: ZL 2011100512896, date of authorization announcement: November 28, 2012). In this study, chitosan mixture was blended with Vaseline to prepare a chitosan–Vaseline gauze (CVG) dressing. The miscibility of the blend system and functional group interaction were investigated by electron microscopy and infrared (IR) spectroscopy. Characteristics of the dressings, including the surface morphology, cytotoxicity, antibacterial activity, and water retention properties, were evaluated. The wound-healing properties of dressings were also investigated in murine models through macroscopic and histological analyses.

MATERIALS AND METHODS

Materials. High molecular weight (MW ~ 800,000) and low (MW ~ 2000) molecular weight chitosan (deacetylation degree

* Address correspondence to Wei-Qiang Tan, Department of Plastic Surgery, Sir Run Run Shaw Hospital, Zhejiang University School of Medicine, No. 3 Qingchun Rd. East, Hangzhou 310016, P. R. China. E-mail: tanweixxxx@zju.edu.cn
† These authors contributed equally to this work.

of 95%) were obtained from Golden-Shell Pharmaceutical Co (Zhejiang, China). Mixed chitosan solution was made in our own laboratory. Sterile gauzes were obtained from Hainuo Medical Technologies Co (Qingdao, China). All other materials were obtained from Gibco Co (Thermo Fisher Scientific, Waltham, MA) unless otherwise noted.

Fabrication of wound dressings. A 3.0% mixed chitosan solution was prepared by dissolving chitosan powder (MW ~ 2000 and ~ 800,000, 1:1, w/w) in 1.0% glacial acetic acid solution (v/v), followed by vigorous stirring overnight to achieve dissolution and then filtered to sterilize. To fabricate chitosan gauze (CG), sterile gauze was soaked in chitosan solution for 24 hours and dried at 60–65°C for 1 hour to evaporate the excess water. To fabricate VG and CVG, the medical Vaseline and paraffin oil were mixed in advance (2:1, w/w) and sterilized by autoclaving. Then dried sterile gauze or CG was soaked in mixed vaseline–paraffin oil for 5 minutes.

Scanning electron microscopy (SEM). The surface characteristics of these dressings were investigated by using a scanning electron microscope (SEM, S-3000N; Hitachi, Tokyo, Japan). Thick layers of gold were used to provide the conduction for the dressings.

Infrared spectroscopy. The IR spectra of membranes were recorded on a Perkin–Elmer IR System Spectrum GX in the range of 4,000–400 cm^{-1} with a resolution of 4 cm^{-1} and averaged over 32 scans.

Cytotoxicity. National Institutes of Health (NIH) 3T3 mouse embryonic fibroblast cells were purchased from the cell bank of the Chinese Academy of Science. Approximately 10×10^3 cells were dispensed into each well of 96-well plates. Different kinds of dressings (CVG, VG, and untreated gauze) were then cut into designated sizes (1.0×1.0 cm^2) and soaked in 10 mL of cell culture medium at 37°C for 24 hours to form the experimental extracts of chitosan and Vaseline. The cells were treated with different concentrations (10, 50, and 100%) of the extract of each dressing and incubated in the presence of 5% CO2 with 95% humidity at 37°C for 24 hours. Cells cultured in 100% cell culture medium without the study dressing (extracts of untreated gauze) were used as negative control group. Cell adhesion and proliferation was visualized using an inverted light microscope (CKX41SF, OLMPUS). Cell activity of NIH3T3 cells was measured after 1.5 hours with a Cell Counting Kit-8 (CCK-8) (Dojindo, Kumamoto, Japan).

The cytotoxicity was evaluated by the relative growth rate (RGR), which was calculated according to the following formula: RGR = the value of the experimental group/the value of the blank control group × 100%. The relationship between RGR and cytotoxicity grade was classified by the GB/T 16175–2008 (the national standard of China about biological evaluation test methods for medical organic silicon materials). If RGR is greater than 100%, the toxicity level is 0. If RGR is between 75% and 99%, the toxicity level is 1. For RGR between 50% and 74%, the toxicity level is 2; level 3 for RGR between 25% and 49%, and level 4 for RGR between 1% and 24%. If RGR is 0, the toxicity level is 5. In the national standard, cytotoxicity evaluation can be considered to meet the criteria of no cytotoxicity at level 0 or 1.

Antibacterial studies. Antibacterial properties of the dressings were evaluated by using the American Association of Textile Chemists and Colorists test method, with some modifications.[17] Briefly, our methods were as follows: nutrient agar, *Staphylococcus aureus*, and *Escherichia coli* were supplied by the Clinical Laboratory Department, the First Affiliated Hospital, College of Medicine, Zhejiang University. Nutrient agar plates were prepared by dissolving 28 g of nutrient agar in 1 L distilled water, and the pH was adjusted to 7. The contents were sterilized by autoclaving at 15 lbs pressure (~120°C) for 20 minutes. The medium when still hot, was poured in sterile plates (approximately 20 mL) allowed to cool so that the agar solidified. The composition of nutrient agar medium was 5 g/L of peptic digest of animal tissue, 5 g/L of sodium chloride, 1.5 g/L of beef extract, 1.5 g/L of yeast extract, and 15 g/L of agar.

Sterile gauzes soaked in penicillin (PE, 80 U in 10 mL of normal saline) and streptomycin (ST, 100 U in 10 mL of normal saline) were used as positive controls, whereas sterile gauzes soaked in 1% acetic acid and chitosan solution were used as negative and blank controls. Bacteria (0.5 MacFarland Standard) were streaked onto the agar surface with a swab. The plates were then divided into five equal sections, labeled for *S. aureus* and *E. coli.* Samples of different types of dressings were then placed at the center of each section and pressed lightly onto the agar. Then the plates were incubated in the inverted position at 37°C for 24 hours.[18] After that, the zone of inhibition around each dressing was measured.

Animals. Adult male Sprague–Dawley (SD) rats (weighing approximately 200–250 g, 8–14 weeks old) were provided by the Laboratory Animal Research Center of the First Affiliated Hospital of Zhejiang University, Hangzhou, China. The animal protocols were approved by the Ethics Committee of the First Affiliated Hospital, College of Medicine, Zhejiang University, and were performed according to the eighth edition of the *Guide for the Care and Use of Laboratory Animals* (NIH Publications, revised 2011).

Water retention measurement. The water content of skin was determined using a Corneometer (Technology of Golden Light, Shenzhen, China) to measure the difference in moisture content of the skin before and after application of the dressings. During the study, sterile gauze, CG, and VG groups were used as the control groups and CVG group as the experimental group. Six male SD rats in each group were used in this experiment. Before the test, the rats were given time to adapt to room conditions, then they were anesthetized with 2% (20 g/L) pentobarbital sodium (30–50 mg/kg) and the dorsal hair was removed. Four test locations (2×2 cm^2) were labeled with a marker pen on the dorsal skin of the rats and covered with an equal-sized piece (2×2 cm^2) of the dressings. All measurements were taken at exactly the same sites. In the first instance, the humidity level of the skin was measured without any application of dressings, and this was used as the baseline water content (H_0). After application of the different dressings, water content of the skin (H_n) was measured with the Corneometer at different time points (3, 6, 12, 24, and 48 hours). Each experiment was conducted in triplicate. The differences in water retention before and after application of dressings were calculated using the following equation:

$$P_n \cdot (\%) \cdot = \cdot (H_n - H_0) / \cdot H_0 \cdot \times \cdot 100 \cdot (n \cdot = \cdot \text{different} \cdot \text{time} \cdot \text{point}),$$

where P_n is the increase in water content at different time intervals after application of dressings compared with that before application, H_n is the water content at different time intervals, H_0 is the water content before application of dressings (baseline water content).

Wound model. A total of 16 male SD rats were used in this experiment, and they were randomly grouped by the random

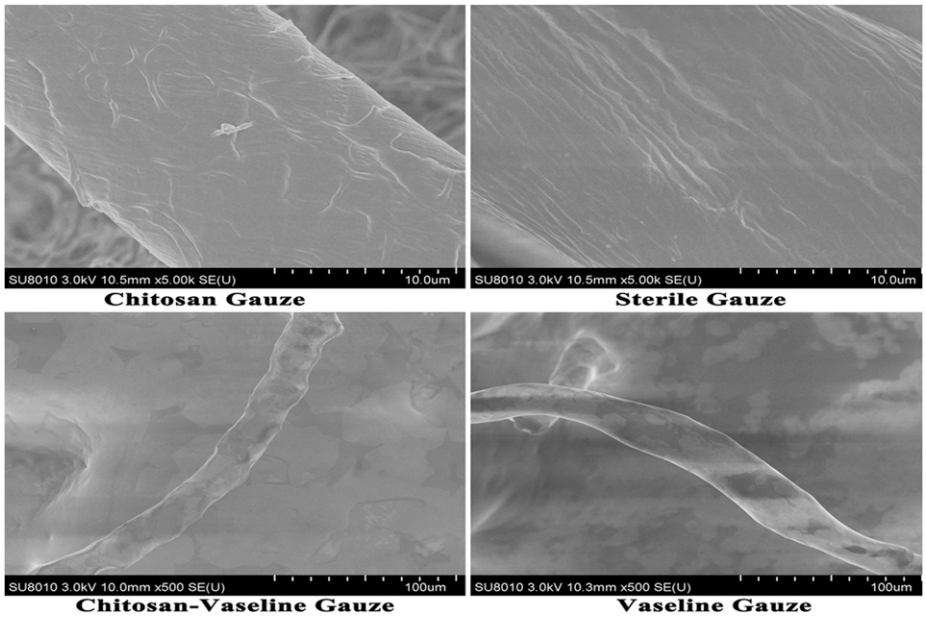

FIGURE 1. Scanning electron microscopy images of dressings: (**A**) chitosan gauze, (**B**) sterile gauze, (**C**) chitosan–Vaseline gauze, and (**D**) Vaseline gauze.

number table (N = 8 for each group). The skin from the back of each rat was prepared by shaving the desired area using electric clipper. After washing the area by 70% ethyl alcohol, two full-thickness round wounds of 2.0 cm diameter down to the panniculus carnosus were created on the skin at sites parallel and equidistant from the vertebral column using a surgical scissor and scalpel. The dimension of the wound site was measured by the digital caliper. Then the wounds of rats were covered with a 2.5 × 2.5-cm piece of CVG or VG. In half of the rats (group A), CVG was applied on the left side and VG on the right side, and in the other half (group B), the dressings were switched. The dressings were changed every 3 days until the wounds healed. The endpoint of healing was set at 100% re-epithelialization. On postoperative days 3, 7, and 14, unhealed wound dimensions were measured blindly, and wound tissues were sampled to allow pathological evaluation.

Gross observation of healing wounds. On the 3rd, 7th, and 14th post-wounding days, gross observation was performed in each rat. After carefully removing the dressing, images were captured by a digital camera (Nikon D610, Japan) to record and analyze the healing and size changes of the wounds. Then the wound outline was first copied to a transparent sheet. After that, a grid was used to count the number of squares and calculate the sizes of the wound sites.

Histology. A strip of tissue containing the wound center and normal skin was obtained. Tissue specimens at different time points were embedded in paraffin wax, sectioned at a thickness of 5 μm, and stained by hematoxylin–eosin (H&E) and Masson's trichrome to visualize the neotissue formation, collagen deposition, and amount of neovasculature.

Immunohistochemical staining (IHC). To investigate the formation of neovessels during the process of wound healing, IHC of CD31 was performed. The positive areas were observed under a microscope (DM2500, Leica) at a fixed

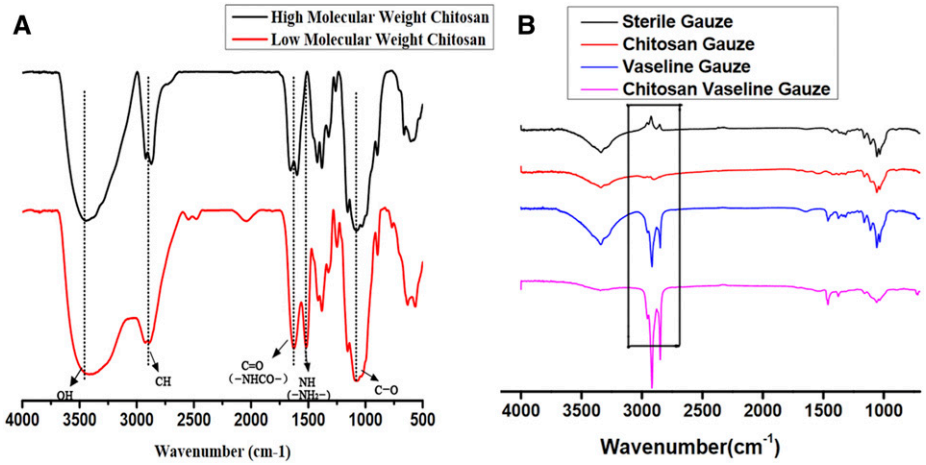

FIGURE 2. Infrared spectrum of (**A**) high and low molecular weight chitosan powders (**B**) samples of chitosan–Vaseline gauze, Vaseline gauze, chitosan gauze, and sterile gauze. This figure appears in color at www.ajtmh.org.

TABLE 1
Cytotoxity detection in various concentrations of extracts ($N = 6$)

Groups	Extract concentration (%)	450 nm absorbance value ($\bar{x} \pm s$)	Relative growth rate (%)	Cytotoxicity grade
Chitosan–Vaseline gauze	100	1.52 ± 0.20	96	1
	50	1.60 ± 0.37	101	0
	10	1.78 ± 0.36	112	0
Vaseline gauze	100	1.38 ± 0.15	87	1
	50	1.40 ± 0.13	89	1
	10	1.53 ± 0.13	97	1
Untreated gauze	–	1.58 ± 0.11	100	0

magnification (×100) to identify the area with the highest vascular density. Then, five non-overlapping fields of fixed magnification (×400) were chosen randomly and images were saved. The relative area of stained neovessels in each image was measured and recorded automatically by the "Count/Size" tool of Image-Pro Plus 6.0.[19,20]

Statistical analysis. SPSS version 21.0 statistical package (IBM Corp., Chicago, IL) was used for data analysis. Normality and homogeneity of the variables were checked first. Comparisons of means of several groups were performed using one-way Analysis of Variance (ANOVA). Comparisons of the differences between two groups were analyzed using Student's *t*-test. A P-value < 0.05 indicated a significant difference between the two groups.

RESULTS AND DISCUSSION

The aim of our study was to develop chitosan and Vaseline–coated sterile gauze with improved properties for wound dressing application. Sterile gauze is used as a support layer for the chitosan–Vaseline mixture. The earlier studies showed that high molecular weight chitosan exerts more potent antibacterial activity against Gram-positive *S. aureus*, whereas low molecular weight chitosan exerts better antibacterial activity against Gram-negative *E. coli* as well as moisture retention.[21,22] Thus, we used chitosan mixture as the basic material, blended with Vaseline. The effects of adding Vaseline to chitosan mixture, bioactive performance, and tissue compatibility of the dressing were investigated by various tests in this study.

Morphology of dressings. As illustrated in Figure 1, surface morphologies of different dressings were evaluated using SEM micrographs. In the high-magnification image of CG, reticulation surrounding the sterile gauze was obviously visible compared with the sterile gauze. However, reticulation in CVG could not be clearly observed. Compared with VG, the structure of CVG showed an uneven morphology. So further, we used IR spectroscopy to investigate the miscibility of these dressings and functional group interaction in them.

The representative bands of chitosan were evident in IR spectroscopy, denoted by arrows, with reference to their pristine materials[23] (Figure 2A). Compared with the sterile gauze, a peak at 2,871 cm^{-1} originating from the vibration of C–H in chitosan was detected in CG (Figure 2B), indicating the successful incorporation of chitosan into sterile gauze. Simultaneously, split peaks between 2,750 and 3,000 cm^{-1} were observed in VG. Compared with VG, the split peaks in CVG were much stronger. It could be inferred that chitosan and Vaseline co-contributed to the stronger split peaks in the CVG.

Cytotoxicity. To investigate the applicability of our new dressings for biomedical applications, the in vitro studies were first performed to evaluate the cytocompatibility of these dressing extracts. NIH3T3 cells at the same initial density were seeded in the 96-well plates and added with different dressing extracts. After 24 hours, cell adhesion and proliferation were visualized using an inverted light microscope. It could be observed in all groups that fibroblast cells adhered to and grew in the vicinity of the dressings. Furthermore, the cell activity was measured by CCK-8 and all the RGR were calculated (Table 1, Supplemental Figure 1). The toxicity grades of all the experimental groups were at level 0 or 1, which can be considered to meet the criteria of non-cytotoxicity. These results obviously suggested that our new dressing extracts did not affect cell viability and this combination would not have an acute cytotoxic effect.

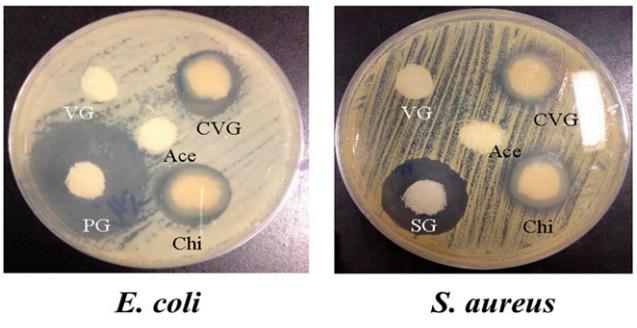

FIGURE 3. Zone of inhibition studies of dressings against *Escherichia coli* (left) and *Staphylococcus aureus* (right). Ace = acetic acid gauze; Chi = chitosan dressing; CVG = chitosan–Vaseline gauze; PG = penicillin gauze; SG = streptomycin gauze; VG = Vaseline gauze. This figure appears in color at www.ajtmh.org.

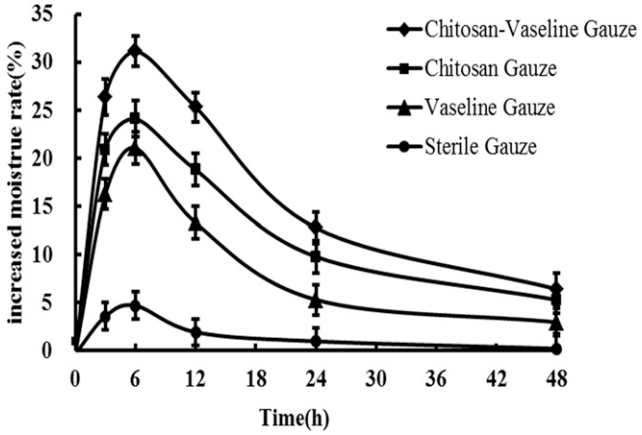

FIGURE 4. Increased moisture rate at different time points after the application of dressings. The increased moisture of chitosan–Vaseline gauze was statistically higher than other groups at 3, 6, 12, 24, and 48 hours (ANOVA, $P < 0.05$).

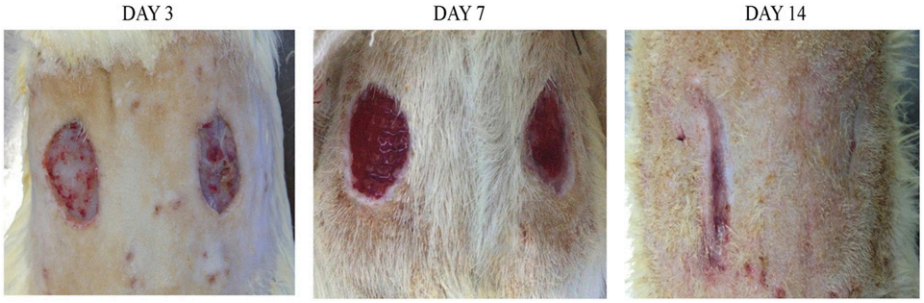

FIGURE 5. Typical photographs of macroscopic appearance of wound repair covered with Vaseline gauze (left) and chitosan–Vaseline gauze (right) at different healing times. This figure appears in color at www.ajtmh.org.

Antibacterial activity (inhibition zone test). The dressings were placed in the plates which were inoculated by *E. coli* or *S. aureus* for 24 hours. Then, a distinct zone of inhibition was observed, which can show the antibacterial activities of the dressings. No zone of inhibition was observed around VG (control) for both *E. coli* and *S. aureus*. The acetic acid dressing (control) were also completely surrounded by bacterial colonies (Figure 3). However, CG, CVG, and the positive control showed obvious surrounding inhibition zones.

We consider that chitosan, which is known for its antibacterial nature, plays an important role in this test as it is one of the constituents of CG and CVG dressings. We did not see any bacterial growth on the surface of those dressings, suggesting that they exercised the bactericidal effects. These results of the antibacterial assay clearly indicated our new dressings' antibacterial activities.

Water retention measurement. It is well known that keeping wounds moist and clean has a beneficial effect on the repair of wound sites. Dressings should keep the wound moist to favor healing and ensure solubilization of antibacterial agents.[24] Thus, we performed the water retention assay by applying dressings on the rat back skin and measuring the water content rate by a Corneometer. The results showed that all the moisture values of rat skin increased after applying the dressings compared with those at 0 hours time point (Figure 4). The increase in moisture in the CVG group was much faster and significantly higher than other groups ($P < 0.05$) at time points 3, 6, 12, and 24 hours. All the findings suggested that our new dressings had good moisture retention properties.

Gross observation of healing wounds. The evaluation of wound healing was performed in rat transcutaneous full-thickness dermal wounds. Gross observation was used to directly compare the healing patterns in this study and the easiness of removing dressings from the wounds was also evaluated when changing the dressings. All 16 animals achieved 100% re-epithelialization by the end of the study. No infection or allergic reactions occurred in this study. Figure 5 shows a series changes of wound beds after the application of different dressings. The healing patterns (Figure 6, 12 wounds of six rats in each group) showed that topical application of CVG facilitated wound closure significantly (*t*-test, $P < 0.05$) from day 3 to day 14, comparing with the control group. Besides, the time for 100% re-epithelialization was significantly shorter in CVG groups than in the VG groups (14.83 ± 0.75 days versus 18.50 ± 0.55 days, *t*-test, $P = 0.00$)

The freshly excised wound surface was easy to be adhered by the wound dressings, and the dressings also have the ability to absorb the exudate from the wound surface.[3,25] When we evaluated the easiness of removing dressings, we found it was hard to perform with quantitative analysis, as it was subjective. Thus, we just described qualitatively here. We found our new dressings were easy to remove from the wounds.

Hematoxylin–eosin and Masson's trichrome staining. At different time points, the tissue specimens treated with different dressings were harvested for histological analysis. During necropsy, there was no microorganism observed in skin lesions of the rats, and no pathological abnormalities were observed in their brains, lung, heart, liver, kidney, and spleen. The results of H&E and Masson's staining are shown in Figures 7 and 8, respectively.

On the 3rd postoperative day, abundant inflammatory cells, capillary buds, and neovessels were observed in both the groups and the proliferation of fibroblasts was also obvious. On the 7th postoperative day, there were still visible inflammatory cells in CVG group, but relatively sparse. We observed an increase in new capillaries and fibroblasts in both groups. The VG group showed presence of angiogenesis and proliferation of fibroblasts to a small degree. On the 14th postoperative day, we observed that there were increased neovessels and fibroblast proliferation in the VG group, whereas there were decreased neovessels and fibroblast proliferation in the CVG group. In addition, re-epithelialization was found in the boundary area around the wounds.

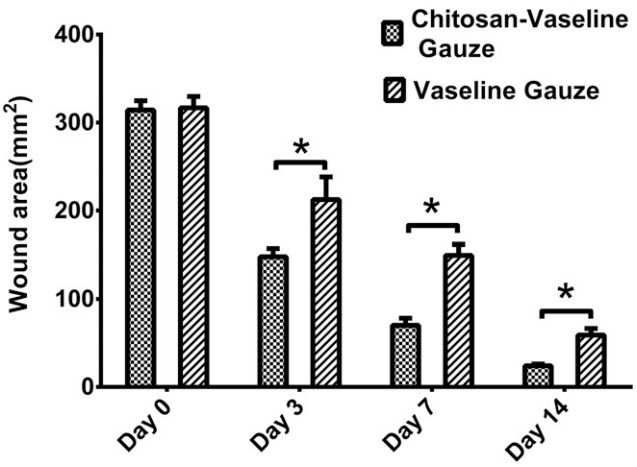

FIGURE 6. Quantitative analysis in gross observation for healing wounds. * indicates a statistically significant difference, $P < 0.05$ (*t*-test).

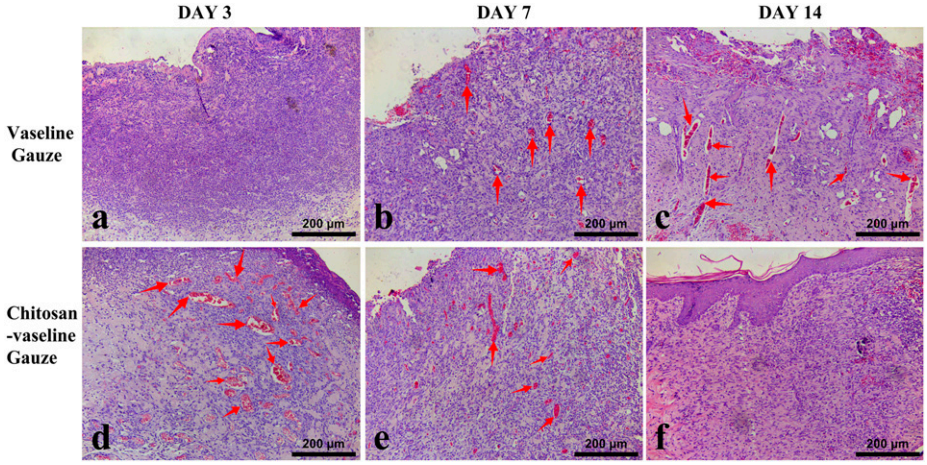

FIGURE 7. Hematoxylin–eosin (H&E) staining of wound tissues of chitosan–Vaseline gauze and Vaseline gauze group for 3, 7, and 14 days after operation. Red arrows indicate blood vessels. This figure appears in color at www.ajtmh.org.

In both groups, collagen deposition was distributed in the granulation tissue and became more abundant with prolongation of the time after surgery (Figure 7 and 8). The morphology of collagen was cotton-like, especially in the early stages (days 3 and 7), whereas on day 14, the arrangement of collagen was relatively thick, irregular, and twisted into spirals in the VG group and this was accompanied by a large number of neovessels. Meanwhile, in the CVG group, the newly formed collagen aggregations appeared as streaks or masses in the wounds on Days 3 and 7. By Day 14, collagen fibers in the CVG groups were thin and arranged in an orderly fashion. The morphology and distribution of new collagen fibers in the CVG group approximated those in the normal dermis.

Immunohistochemical staining. The number of endothelial cells is one of the most significant part of the formation of neovessels during the process of wound healing, which could be measured by IHC of CD31.[26] Thus, we performed IHC in these groups. Endothelial cells appeared brown by CD31 IHC staining (Figure 9), as seen by light microscopy. Figure 10 showed neovessel density as measured using image software (relative area), where the CVG group showed a declining trend, whereas the VG group showed a rising trend in a time-dependent manner. The vascular density in the CVG group was much higher than that in the VG group on Day 3. By Day 7, the number of neovessels in the CVG group declined, whereas it rose in the VG group. On Day 14, the blood vessels were abundantly distributed throughout the granulation tissue in the VG group compared with the CVG group ($P < 0.05$). The results of CD31 IHC were in agreement with those shown in H&E and Masson's trichrome stainings.

In rat model, the smaller wound beds and shorter 95% re-epithelialization time in the CVG groups demonstrated that the CVG dressing significantly promoted wound healing. During the healing period, histological evidence and the result of IHC staining revealed that in the CVG group, collagen fibers were thin and arranged in an orderly fashion, and the number of neovessels markedly decreased. A plausible explanation is as follows: after the wound dressings were applied to the wounds, the loaded constituents (chitosan and Vaseline) then gradually released. They might provide a nonprotein matrix for tissue growth, activate macrophages for antibacterial activity, and stimulate cell proliferation and histoarchitectural tissue organization. Furthermore, chitosan gradually depolymerized to release N-acetyl-β-D-glucosamine, which could initiate fibroblast proliferation, stimulate natural hyaluronic acid synthesis,

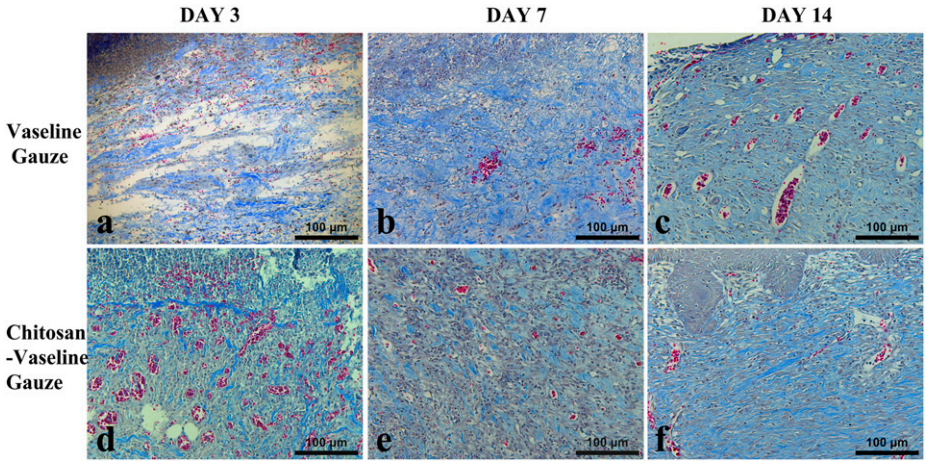

FIGURE 8. Masson's trichrome staining of wound tissues of chitosan–Vaseline gauze and Vaseline gauze group on postoperative days 3, 7, and 14. The blue areas indicate the sites of collagen deposition. This figure appears in color at www.ajtmh.org.

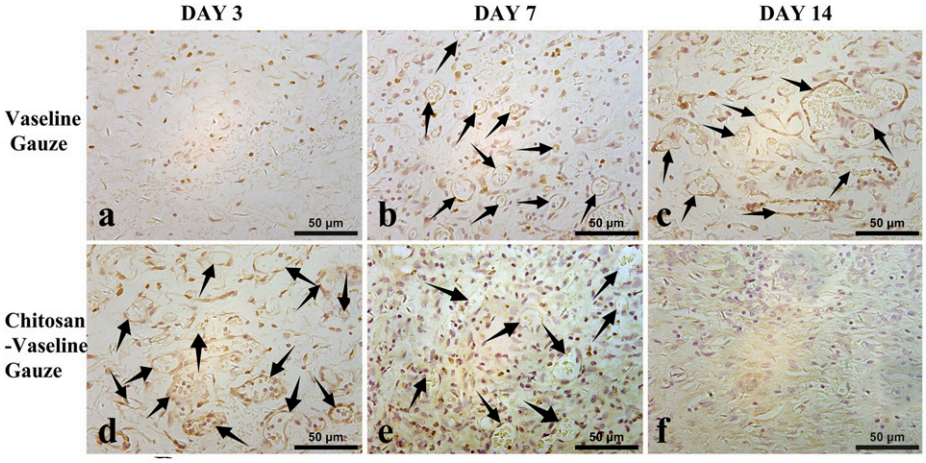

FIGURE 9. CD31 immunohistochemical staining of tissues slices of the wounds treated by chitosan–Vaseline gauze and Vaseline gauze on postoperative days 3, 7, and 14. Black arrows indicate blood vessels. This figure appears in color at www.ajtmh.org.

and help in ordered collagen deposition at the wound site.[7] Vaseline might act as a moisture insulator for local wound conditions. Chitin-based dressings can accelerate repair of different tissues by facilitating the contraction of wounds as well as regulating the secretion of some inflammatory mediators such as prostaglandin E, interleukin 1, and interleukin 8.[7,27] We hypothesized that chitosan and Vaseline also accelerated the remodeling and expansion of the vascular network as the expression levels of blood vessels were significantly influenced by applying the CVG. The faster and functional angiogenesis in the CVG group improved the delivery of nutrients and oxygen to the cells at the wound sites. On the 14th day, the number of neovessels was much less in the CVG group possibly because the newly formed blood vessels become more mature. Thus, all the aforementioned factors together contributed to faster wound healing.

CONCLUSION

The observations of the study suggest that chitosan–Vaseline dressing is effective in animal models of wound healing and has the potential as a wound care material for future development. Considering the longer healing period of chronic wounds, patients should be provided the correct dressing, which is curative and cost-effective.[28] It is also noteworthy that chronic wounds are dynamic in presentation, and dressings that can optimize each stage in the healing process should be further evaluated. Furthermore, studies will be required to focus on delineating the mechanisms promoting the wound healing and evaluating the effectiveness of the dressings in preventing hypertrophic scars or other skin conditions.

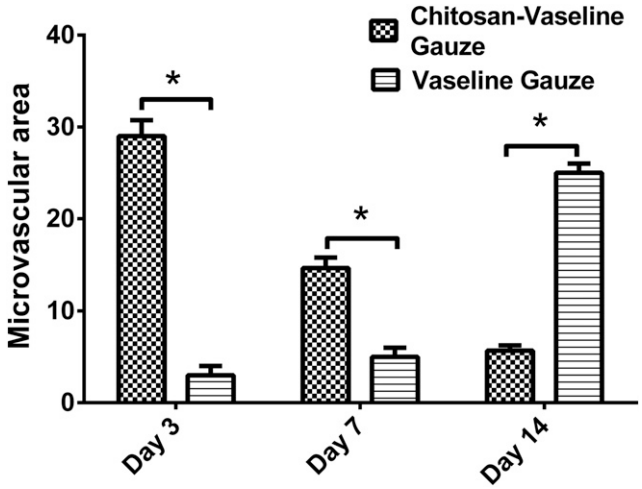

FIGURE 10. Density of blood vessel measurement in the tissues slices of the wounds treated by chitosan–Vaseline gauze and Vaseline gauze for 3, 7, and 14 days after operation. * Indicates statistically significant difference, $P < 0.05$ (*t*-test).

Received May 21, 2019. Accepted for publication October 29, 2019.

Published online December 2, 2019.

Note: Supplemental figure appears at www.ajtmh.org.

Financial Support: This study was supported by the National Natural Science Foundation of China (No. 81671918 and 81372072), the National Key Research Program of China (2016YFC1101004), and Zhejiang Provincial Medical and Healthy Science Foundation of China (No. 2019ZD028 and 2018KY874).

Authors' addresses: Qing-Qing Fang, Xiao-Feng Wang, Wan-Yi Zhao, and Wei-Qiang Tan, Department of Plastic Surgery, Sir Run Run Shaw Hospital, Zhejiang University School of Medicine, Hangzhou, P. R. China, E-mails: 11618208@zju.edu.cn, 11818375@zju.edu.cn, 21718412@zju.edu.cn, and tanweixxxx@zju.edu.cn. Bang-Hui Shi, Chun-Ye Chen, and Min-Xia Zhang, Department of Plastic Surgery, The Fourth Affiliated Hospital, Zhejiang University School of Medicine, Yiwu, P. R. China, E-mails: 3090103932@zju.edu.cn, zella02@sina.com, and lanxiechen926@163.com. Dong Lou and Lie Ma, Department of Polymer Science and Engineering, Zhejiang University, Hangzhou, P. R. China, E-mails: ldld332211@126.com and liema@zju.edu.cn. Xiaozhi Wang, College of Information Science and Electronic Engineering, Zhejiang University, Hangzhou, P. R. China, E-mail: xw224@zju.edu.cn.

REFERENCES

1. Holmes CJ, Plichta JK, Gamelli RL, Radek KA, 2015. Dynamic role of host stress responses in modulating the cutaneous microbiome: implications for wound healing and infection. *Adv Wound Care (New Rochelle) 4:* 24–37.
2. Alemdaroğlu C, Değim Z, Çelebi N, Zor F, Öztürk S, Erdoğan D, 2006. An investigation on burn wound healing in rats with chitosan gel formulation containing epidermal growth factor. *Burns 32:* 319–327.
3. Ribeiro MP et al., 2009. Development of a new chitosan hydrogel for wound dressing. *Wound Repair Regen 17:* 817–824.

4. Dai T, Tegos GP, Burkatovskaya M, Castano AP, Hamblin MR, 2009. Chitosan acetate bandage as a topical antimicrobial dressing for infected burns. *Antimicrob Agents Chemother 53:* 393–400.
5. Robson MC, 1997. Wound infection. A failure of wound healing caused by an imbalance of bacteria. *Surg Clin North Am 77:* 637–650.
6. Dai T, Tanaka M, Huang YY, Hamblin MR, 2011. Chitosan preparations for wounds and burns: antimicrobial and wound-healing effects. *Expert Rev Anti Infect Ther 9:* 857–879.
7. Jayakumar R, Prabaharan M, Sudheesh Kumar PT, Nair SV, Tamura H, 2011. Biomaterials based on chitin and chitosan in wound dressing applications. *Biotechnol Adv 29:* 322–337.
8. Pereira RF, Bartolo PJ, 2016. Traditional therapies for skin wound healing. *Adv Wound Care 5:* 208–229.
9. Anjum S, Gupta A, Sharma D, Gautam D, Bhan S, Sharma A, Kapil A, Gupta B, 2016. Development of novel wound care systems based on nanosilver nanohydrogels of polymethacrylic acid with Aloe vera and curcumin. *Mater Sci Eng C Mater Biol Appl 64:* 157–166.
10. Xu F, Weng B, Gilkerson R, Materon LA, Lozano K, 2015. Development of tannic acid/chitosan/pullulan composite nanofibers from aqueous solution for potential applications as wound dressing. *Carbohydr Polym 115:* 16–24.
11. Anjum S, Arora A, Alam MS, Gupta B, 2016. Development of antimicrobial and scar preventive chitosan hydrogel wound dressings. *Int J Pharm 508:* 92–101.
12. Haik J, Kornhaber R, Blal B, Harats M, 2017. The feasibility of a handheld electrospinning device for the application of nanofibrous wound dressings. *Adv Wound Care (New Rochelle) 6:* 166–174.
13. Ong SY, Wu J, Moochhala SM, Tan MH, Lu J, 2008. Development of a chitosan-based wound dressing with improved hemostatic and antimicrobial properties. *Biomaterials 29:* 4323–4332.
14. Zhang D, Zhou W, Wei B, Wang X, Tang R, Nie J, Wang J, 2015. Carboxyl-modified poly(vinyl alcohol)-crosslinked chitosan hydrogel films for potential wound dressing. *Carbohydr Polym 125:* 189–199.
15. Huang SH, Yang PS, Wu SH, Chang KP, Lin TM, Lin SD, Lai CS, Lee SS, 2010. Aquacel Ag with Vaseline gauze in the management of toxic epidermal necrolysis (TEN). *Burns 36:* 121–126.
16. Huang SH, Lin CH, Chang KP, Wu SH, Lin SD, Lai CS, Ou SF, Lee SS, 2014. Clinical evaluation comparing the efficacy of aquacel Ag with vaseline gauze versus 1% silver sulfadiazine cream in toxic epidermal necrolysis. *Adv Skin Wound Care 27:* 210–215.
17. Wang CC, Su CH, Chen CC, 2008. Water absorbing and antibacterial properties of N-isopropyl acrylamide grafted and collagen/chitosan immobilized polypropylene nonwoven fabric and its application on wound healing enhancement. *J Biomed Mater Res A 84:* 1006–1017.
18. Haerian-Ardakani A, Rezaei M, Talebi-Ardakani M, Keshavarz Valian N, Amid R, Meimandi M, Esmailnejad A, Ariankia A, 2015. Comparison of antimicrobial effects of three different mouthwashes. *Iran J Public Health 44:* 997–1003.
19. Zhang MY, Ding SL, Tang SJ, Yang H, Shi HF, Shen XZ, Tan WQ, 2014. Effect of chitosan nanospheres loaded with VEGF on adipose tissue transplantation: a preliminary report. *Tissue Eng Part A 20:* 2273–2282.
20. Tan WQ, Gao ZJ, Xu JH, Yao HP, 2011. Inhibiting scar formation in vitro and in vivo by adenovirus-mediated mutant Smad4: a preliminary report. *Exp Dermatol 20:* 119–124.
21. Younes I, Rinaudo M, 2015. Chitin and chitosan preparation from marine sources. Structure, properties and applications. *Mar Drugs 13:* 1133–1174.
22. Younes I, Sellimi S, Rinaudo M, Jellouli K, Nasri M, 2014. Influence of acetylation degree and molecular weight of homogeneous chitosans on antibacterial and antifungal activities. *Int J Food Microbiol 185:* 57–63.
23. Cheung RC, Ng TB, Wong JH, Chan WY, 2015. Chitosan: an update on potential biomedical and pharmaceutical applications. *Mar Drugs 13:* 5156–5186.
24. Sahraro M, Yeganeh H, Sorayya M, 2016. Guanidine hydrochloride embedded polyurethanes as antimicrobial and absorptive wound dressing membranes with promising cytocompatibility. *Mater Sci Eng C Mater Biol Appl 59:* 1025–1037.
25. Azad AK, Sermsintham N, Chandrkrachang S, Stevens WF, 2004. Chitosan membrane as a wound-healing dressing: characterization and clinical application. *J Biomed Mater Res B Appl Biomater 69:* 216–222.
26. Kajbafzadeh AM, Sabetkish S, Tourchi A, Amirizadeh N, Afshar K, Abolghasemi H, Elmi A, Talab SS, Eshghi P, Mohseni MJ, 2014. The application of tissue-engineered preputial matrix and fibrin sealant for urethral reconstruction in rabbit model. *Int Urol Nephrol 46:* 1573–1580.
27. Patel S, Goyal A, 2017. Chitin and chitinase: role in pathogenicity, allergenicity and health. *Int J Biol Macromol 97:* 331–338.
28. Dabiri G, Damstetter E, Phillips T, 2016. Choosing a wound dressing based on common wound characteristics. *Adv Wound Care 5:* 32–41.